Magnetite nanoparticles enhance the bioelectrochemical treatment of municipal sewage by facilitating the syntrophic oxidation of volatile fatty acids

Carolina Cruz Viggi[1], Stefania Casale[1], Habib Chouchane[2], Refka Askri[2], Stefano Fazi[1], Ameur Cherif[2],Marco Zeppilli[3], Federico Aulenta[1,*]

[1] Water Research Institute (IRSA), National Research Council (CNR), via Salaria km 29,300, 00015 Monterotondo, Italy

[2]Univeristy ofManouba, ISBST, BVBGR-LR11ES31, Biotechpole Sidi Thabet, 2020, Ariana, Tunisia

[3]Department of Chemistry, Sapienza University of Rome, P.Le Aldo Moro 5, 00185, Rome, Italy

* Corresponding Author

E-mail: aulenta@irsa.cnr.it; Tel: +39-0690672751; Fax: +39-0690672787

Abstract

Microbial electrochemical technologies (METs) represent a novel technological platform to harvest the energy trapped in municipal wastewater while simultaneously cleaning up the wastewater. At the anode of METs, electro-active bacteria(EAB) anaerobically oxidize wastewater constituents using the electrode as the terminal electron acceptor and, by so doing, generate an electric current. To convert complex wastewater constituents into electricity EAB must establish cooperative and syntrophic metabolic relationships with other members of the microbial community (e.g., fermentative bacteria), as well as must compete with methanogens for consumption of hydrogen and acetate.

Here, we examined the addition of magnetite nanoparticles (250 mg Fe/L) as a novel strategy to manipulate such metabolic activities and in turn maximize the efficiency of wastewater treatment and the yield of electric current generation. Batch experiments carried out either in the presence of a mixture of volatile fatty acids or of a synthetic sewage demonstrated that magnetite addition accelerate the rate of electrogenic oxidation of specific compounds, particularly propionate (up to 120%), an intermediate which frequently accumulates during anaerobic treatment processes, while correspondingly enhancing electric current generation (up to 90%) and diminishing the rate of competing methane generation (up to 50%).

Notably, the composition of the microbial community (suspended an attached onto the electrode surface) was not substantially affected by the presence of magnetite nanoparticles, possibly suggesting that these latter simply facilitated extracellular electron transfer mechanisms (among microbes and with the electrode), rather

than enriched for specific microorganisms. Although further work is certainly needed to shed light on the working mechanisms of the process, it is apparent that magnetite addition may represent a viable strategy to kick-start a bioelectrochemical system designed for wastewater treatment and improve, at least on a short-term scale, the effectiveness of electrogenic substrate oxidation processes.

1. Introduction

In recent years, sustainable treatment, valorizationand re-use of municipal wastewater are receiving considerable attention due to the growing shortage of freshwater resources, depletion of fossil fuel, and diffuse environmental pollution. At present, municipal wastewater treatment is typically accomplished by means of aerobic treatment processes, such as the activated sludge technology, which however consume substantial amounts of non-renewable energy, especially when designed to achieve nitrification, and cause environmental concerns due to, among the others, the release in the atmosphere of greenhouse gases like nitrous oxide and carbon dioxide.

On the other hand, recent studies have pointed out that the (chemical) energy stored within municipal wastewater is, at least in large centralized plants, up to 10-times the energy consumed for its (aerobic) treatment[1,2]. This suggests that a transition from aerobic to anaerobic treatment technologies could, in principle, provide the opportunity for turning municipal wastewater treatment facilities from net-users to net-contributors of energy or, at least, for reducing the overall costs and the environmental burden of treatment [3].

To date, only few technologies exist that enable coupling municipal wastewater treatment to energy or even chemicals recovery/production. Among them, anaerobic digestion (AD) of sewage sludge (i.e., the new biomass generated from the biodegradation of organic matter) is the only one having commercial application[4,5]. In spite of the continued research efforts, however, the application of AD to the treatment of low-strength (municipal) wastewater at ambient

temperaturesis not yet a feasible and sustainable option[6]. In recent years, microbial electrochemical technologies (METs) have emerged as a noveltechnological platform to harvest the energy trapped in wastewater while simultaneously cleaning up the wastewater[7,8]. METs rely on the activity of, so called, "electro-active bacteria (EAB)", microorganisms which are capable of engaging in extracellular electron transfer reactions with solid-state electrodes[9,10]. At the anode of METs, the electro-active bacteria anaerobically oxidize reduced substrates using the electrode as terminal electron acceptor and, by so doing, generate an electric current which can be harvested or alternatively exploited for the generation (at the cathode) of valuable products such as hydrogen or methane[5,11–14].

The majority of EAB are metabolically restricted to using only simple molecules as electron donors (i.e., sugars, VFAs, alcohols, hydrogen)[15,16]. Hence, in the case of wastewater treatment, EAB rely on the activity of other community members (e.g., hydrolytic, fermentative, and acidogenic bacteria) which break down complex organic constituents contained in wastewater into simpler molecules which can be in turn converted into electricity by EAB [17].

At the same time, since methanogens share the same substrates of EAB (i.e., acetate, hydrogen), methanogenesis is a competing metabolic reaction which may divert electrons away from electric current, thereby diminishing the efficiency of the bioelectrochemical wastewater treatment process [18].

Over the last years, much research efforts have focused on the optimization of the microbe/electrode interface in order to boost the power output of MET via i.)

105 engineering the structure and chemistry of the electrode and ii.) tailoring the
106 biofilm structure/composition[19–21].
107 On the other hand, no effective strategies were identified for effectively
108 manipulating the syntrophic/cooperative relationships which establish between
109 EAB and other microorganismsin order to maximize the efficiency of substrate
110 degradation (i.e., a factor which is critical in the context of wastewater treatment)
111 and the yield of electric current generation.
112 Recent studies have suggested that the electron flow in anaerobic ecosystems can
113 be facilitated through the addition of "electrically conductive" nanoparticles
114 (NPs)which may serve as electrical conduits in the electron transfer between
115 microbial species such as acetogens and methanogens[22–28], as well as between
116 microorganisms and electrode (both anodes and cathodes)[29,30].
117 In this context, in the present study we evaluated whether the addition of
118 magnetite NPs to the anode compartment of a MET could be exploited as a strategy
119 to :i.) improve the electrogenic treatment of substrates requiring syntrophic
120 and/or cooperative metabolisms to be oxidized, such as VFA and synthetic
121 municipal wastewater; ii.) minimize the competition between EAB and
122 methanogens for such substrates (in favor of EAB) thereby improving the efficacy
123 of energy recovery from wastewatertreatment.

2. Materials and Methods

2.1. Synthesis of magnetite nanoparticles

Magnetite nanoparticles were synthesized according to a previously described protocol[31]. Briefly, $FeCl_3$ (5.2 g) and $FeCl_2$ (2.0 g) were dissolved into an acidic (HCl 0.4 M) aqueous solution which was then added dropwise into a 1.5 MNaOH solution under vigorous mixing, generating an instant black precipitate of Fe_3O_4 (magnetite). The precipitate was isolated in the magnetic field, purified by centrifugation, and suspended in 0.25 L of deoxygenated water.

2.2. Source cultures

The inoculum used for bioelectrochemical experiments here in described consisted of an anaerobic methanogenic sludge collected from a lab-scale mesophilic (37 °C) digester fed with food wastes[32].

2.3. Experimental setup

The bioelectrochemical cell setup used in this study consisted of two gastight borosilicate glass bottles (each having a total volume of 270 mL and working volume of 150 mL) separated by a 3-cm^2 cross-sectional area Nafion® 117 proton exchange membrane (PEM)[33]. Prior to its use, the PEM was boiled successively in four separate solutions for 2 hours each:H_2O_2 (3% v/v), deionized (DI) water, 0.5M H_2SO_4 and DI water, and then finally stored in DI water until use. The cathode and anode were graphite rods (6 mm diameter, Sigma Aldrich, Milano, Italy). The nominal surface area of the anode (calculated by taking into account only the part

148 of the electrode that was immersed in the liquid phase) was 9.7 cm^2. The distance
149 between the anode and the cathode was approximately 10 cm. Prior to their use,
150 the graphite electrodes were pretreated as described elsewhere[34]. A reference
151 electrode (KCl-saturated Ag/AgCl,+199 mV vs. the standard hydrogen electrode
152 (SHE); AmelS.r.l., Milano, Italy) was placed in the anodic chamber. The anolyte and
153 catholyte consisted of anaerobic medium, prepared as described below.
154 Electrochemical potentiostatic measurementsand monitoring were carried out by
155 using an IVIUM-n-statmultichannel potentiostat (IVIUM, The Netherlands).
156 Titanium wires (0.81 mm diameter, Sigma–Aldrich, Milano, Italy) were used to
157 connect the graphite electrodes to the cables of the potentiostat. The anolyte and
158 catholyte consisted of anaerobic medium, prepared as described
159 below.Throughout the manuscript, all potentials are reported with respect to SHE.
160
161 *2.4. Bioelectrochemical experiments*
162 The anode and cathode compartments of the bioelectrochemical cells were each
163 filled with 200 mL of mineral medium, which was purged with a N_2/CO_2(70:30
164 v/v) gas mixture to remove the dissolved oxygen and establish anaerobic
165 conditions. The medium contained the following components: NH_4Cl (0.5 g/L),
166 $MgCl_2*6H_2O$ (0.1 g/L),K_2HPO_4(0.4 g/L), $CaCl_2*2H_2O$ (0.05 g/L), trace metal
167 solution (10 mL/L)[35], vitamin solution (10 mL L^{-1})[36].The pH value of the medium
168 was set at 7.5 by using $NaHCO_3$ (10% w/v).
169 At the start of the study, the anode compartment of the two identical cells was
170 inoculated with 5 mL of a methanogenic sludge from a lab-scale anaerobic digester

171 treating food wastes. The resulting initial biomass concentration in the anode
172 compartment of the bioelectrochemical cells was around 400 mgVSS/L.
173 One of the two cells (Cell 1) was supplemented with a suspension of magnetite
174 nanoparticles (5 mL) to a final concentration of 250 mg Fe/L, whereas the other
175 one (Cell 2) was supplemented with a corresponding volume of mineral medium
176 and served as a control.
177 In the first set of experiments, the anode compartment of the two cells was
178 supplemented with a mixture of volatile fatty acids (butyrate 50%, propionate
179 25%, acetate 25%) to a final concentration of approximately 300 mgCOD/L, while
180 the anode was potentiostatically controlled at -100 mV vs. SHE. Once the dose of
181 substrate was nearly completely consumed and the electric current returned to
182 baseline values, the cell was disconnected from the potentiostat and a fixed volume
183 of liquid phase (approximately 50 mL) was removed from each compartment and
184 replaced with fresh anaerobic medium. Prior to commencing a new feeding cycle,
185 both compartments of the cells were purged with the N_2/CO_2(70:30 v/v) gas
186 mixture and the pH adjusted to 7.5 by using $NaHCO_3$ (10% w/v).
187 In the second set of experiments, the anode of the two cells was spiked with a
188 synthetic sewage to a final concentration of approximately 300 mgCOD/L[37], having
189 the following composition: peptone (160 mg/L), meat extract (110 mg/L), urea (30
190 mg/L), NaCl (7 mg/L), $CaCl_2*2H_2O$ (4 mg/L), $MgSO_4*7H_2O$ (2 mg/L), K_2HPO_4 (28
191 mg/L). Also in this case, throughout the experiments the anode was
192 potentiostatically controlled at -100 mV vs. SHE. Once most of the substrate was
193 consumed, the cells were disconnected from the potentiostat and a fixed volume of
194 liquid phase (approximately 50 mL) was removed from each compartment and

195 replaced with fresh anaerobic medium. Prior to commencing a new feeding cycle,
196 both compartments were purged with the N_2/CO_2(70:30 v/v) gas mixture and the
197 pH adjusted to 7.5 by using $NaHCO_3$ (10% w/v).
198 Throughout all the experiments, the cells were maintained at 25 °C, with the liquid
199 phase of each compartment vigorously stirred (400 rpm) with a magnetic stirrer.
200 Over the course of the feeding cycles (both in the first and in the second set of
201 experiments), the liquid phase and the headspace of the cells were regularly
202 sampled with syringes for the determination of the total COD, individual VFAs and
203 methane, respectively. Cells were also monitored for the produced electric current
204 and cumulative electric charge.
205
206 *2.5. Analytical methods and calculations*
207 Volatile fatty acids (i.e., acetate, propionate, butyrate) were analyzed by injecting 1
208 µL of filtered (0.22 µm porosity) liquid sample, pre-acidified with formic acid (to a
209 final concentration of 0.033 mol/L),into a Perkin-Elmer Auto System gas
210 chromatograph(2m × 2mm stainless steel column packed with phase 0.3%
211 Carbowax 20 M, 0.1% H_3PO_4, 60/80 Carbopack C support, Supelco, USA; N_2carrier
212 gas at 20 mL/min;oven temperature at 120 °C; injector temperature at 200 °C;
213 flame ionization detector (FID) temperature at 200 °C).
214 Methane was analyzed by injecting 50 µL of headspace sample (removed from the
215 bottles with a gas tight Hamilton syringe) into a Perkin-Elmer Auto System gas
216 chromatograph [2 m × 2 mm stainless steel column packed with molecular sieve,
217 Supelco, USA; N_2carriergas at 20 mL/min; oven temperature at 150 °C; injector

temperature at 200 °C; thermal conductivity detector(TCD) temperature at 200 °C].

Chemical oxygen demand(COD) was measured on filtered (0.22 μm porosity) liquid samples withMerck® Spectroquant kits. Volatile suspended solids (VSS) were measured according to the standard methods for examination of water and wastewater[38].

The Coulombic efficiency (η, %) (or yield of current production) was calculated as the ratio between the electric charge and the theoretical electric charge which would be generated from the complete oxidation (to carbon dioxide and water) of the removed organic substance (in terms of COD), according to the following equation:

$$\eta(\%) = \frac{\int_0^t i\,dt}{\frac{\Delta COD \cdot V_{an}}{MW\ O_2} \cdot f \cdot F} \cdot 100 \quad (1)$$

where i (mA) is the electric current flowing in the circuit; dt is the time interval under consideration; ΔCOD (mgCOD/L) is the organic substance removed; V_{an} (L) is the total liquid volume in the anode chamber; MW O_2(mg/mmol) is the molecular weight of oxygen; f is the number of mmol of electrons released from the complete oxidation of 1 mmol of oxygen; and F is the Faraday's constant (96485 C/mmol).

The yield of methane production (η_{CH4}, %) was calculated as the ratio between the amount of produced methane (ΔCH_4) and the amount of removed substrate

241 (ΔCOD), both expressed in COD units, in the time interval under consideration,
242 according to the following equation:
243
244 $$\eta_{CH4}(\%) = \frac{\Delta CH_4}{\Delta COD} \cdot 100$$
245 (2)
246
247 *2.6. Chemicals*
248 All the chemicals were analytical grade or higher and used as received.
249
250 *2.7. Molecular and microscopy analysis of the microbial communities*
251 Fluorescence in situ hybridization (FISH) analysis was performed on
252 paraformaldehyde-fixed samples removed from anode compartment of the cells at
253 the end of the first and of the second set of experiments, according to a procedure
254 described elsewhere[39]. Oligonucleotide probes specific for *Bacteria* (EUB338I-III)
255 and *Archaea* (ARC915 probe) domains were used. Details of the employed
256 oligonucleotide probes are available at probeBase[40]. Samples were examined by
257 epifluorescence microscopy (Olympus BX51). All the hybridizations with specific
258 probes were carried out in combination with DAPI staining to estimate the portion
259 of cells targeted by group specific probes out of the total cells. Data were based on
260 10 fields of view per sample, with each sample analyzed in duplicate. The average
261 number of DAPI-stained cells, per field of view, was in the range of 80–100.
262 In order to visualize specific cells within the 3D structure of the aggregates, FISH
263 was combined with confocal laser scanning microscopy (CSLM; Olympus FV1000)
264 [39,41]. The hybridized *Bacteria* cells were excited with the 488 nm line of an Ar laser

Commentato [HC1]: epifluo microscopy results are not included in the results section !

(excitation) and observed in the green channel from 500 to 530 nm (emission). *Archaea* cells were excited with the 543 nm line of a He–Ne laser and observed in the red channel from 550 to 660 nm. Magnetite particles were visualized by their reflection signal (405 nm line of a diodo laser). The three-dimensional reconstruction of CSLM images was elaborated by the software IMARIS 7.6 (Bitplane, Switzerland).

2.8. Illumina Miseq sequencing of 16S rRNA gene analysis

At the end of the first and second set of bioelectrochemical experiments, the anode biofilms and anolytes of cells supplemented or not with magnetite NPs were sampled for microbial communities'analyses. The anaerobic methanogenic sludge used as initial inoculums was also sampled and analyzed.

For each anode to be analyzed, 1 to 2 cm^2 of biofilm binding to the surface was removed aseptically with a scalpel and place it in sterile 2 mL eppendorf tube. 2 mL of sterile distilled water were added, and the suspension was sonicated (2 x 3 min at a power level of 80 W). After centrifugation (16,000 g for 5 min at 4°C), the biofilm was resuspended in 500 µl of sterile lysis buffer (EDTA 40 mM, Tris HCl 50 mM pH 8, Sucrose 0.75 M) for DNA extraction then stored at -20°C. For the anolytes analyses, 50 mL of water samples were aseptically collected in sterile bottles at the end of the experimentation. The water samples were filtered through sterile 0.22 µm nitrocellulose membrane filters using a sterile filtration system. Each filter was subdivided in two parts, wrap aseptically and each half was put in sterile 2 mL Eppendorf tube. Each half filter was added with 1.8 mL of sterile lysis buffer and stored at - 20°C until DNA extraction. Finally, the initial sludge used as

inoculum was collected aseptically, centrifuged at 7,000 g for 7 min at 4°C and re-suspend in 10 mL lysis buffer and store at -20°C until DNA extraction.

Genomic DNA extraction by using NucleoSpin Soil Isolation Kit according the manufacturer's instructions with modifications was performed. Yield and quality of DNA and PCR products were checked by using agarose gel electrophoresis and Nanodrop. Inorder to make an overview of the composition, dynamics and taxonomy of the bacterial communities in the different samples, ~~DGGE and~~ Illumina Miseq sequencing of 16S rRNA genewere performed. The 16S rRNA gene V4 variable region PCR primers 515/806 were used in a single-step 30 cycles PCR using the HotStarTaq Plus Master Mix Kit (Qiagen, USA). Sequencing was performed at MR DNA (www.mrdnalab.com, Shallowater, TX, USA) on an Ion Torrent PGM following the manufacturer's guidelines. Sequences were depleted of barcodes and primers,then sequences <150bp or with ambiguous base calls or with homopolymer runs exceeding 6bpwere all removed. OTUs were then generated and clustering at 97% similarity. OTUs were taxonomically classified using BLASTn against two databases RDPII (http://rdp.cme.msu.edu) and NCBI (www.ncbi.nlm.nih.gov).

Commentato [HC2]: reviewers will bother us on the nature of these modifications, it is then desirable to delete this term, otherwise I can add a few sentences

Commentato [HC3]: in the paper only the results of metagenomics are presented so please delete DGGE

3. Results

The effect of magnetite NPs on the electrogenic oxidation of organic substrates (i.e., a mixture of butyrate, propionate, and acetate or asynthetic municipal sewage) with ananode polarizedat –100 mV vs. SHE serving as the only metabolic electron acceptor was investigated by means of bioelectrochemical batch experiments.The experiments were carried out in two identical H-type bioelectrochemical cells, which were inoculated (at the anode) with a methanogenic sludge. The anode compartment of one of the two cells (Cell 1) was supplemented with a suspension of magnetite nanoparticles (250 mg Fe/L), whereas the other one (Cell 2) was supplemented with a corresponding volume of anaerobic mineral medium and served as a control.

In a first set of batch experiments, the anode of the two cells was periodically spiked with a mixture of volatile fatty acids (butyrate 50%, propionate 25%, acetate 25%, on a COD basis) to a final concentration of approximately 300 mgCOD/L. In a second set of experiments, the anode was periodically spiked with a synthetic municipal sewage, prepared according to the OECD guideline for testing chemicals.

3.1. Bioelectrochemical treatment of a VFA mixture

The first set of experiments consisted of 5 successive fed-batch feeding cycles, in which the anode compartment of the bioelectrochemical cells was supplemented with a mixture of VFA. Figure 1 show the time course of VFA and methane concentrations during the first feeding cycle.

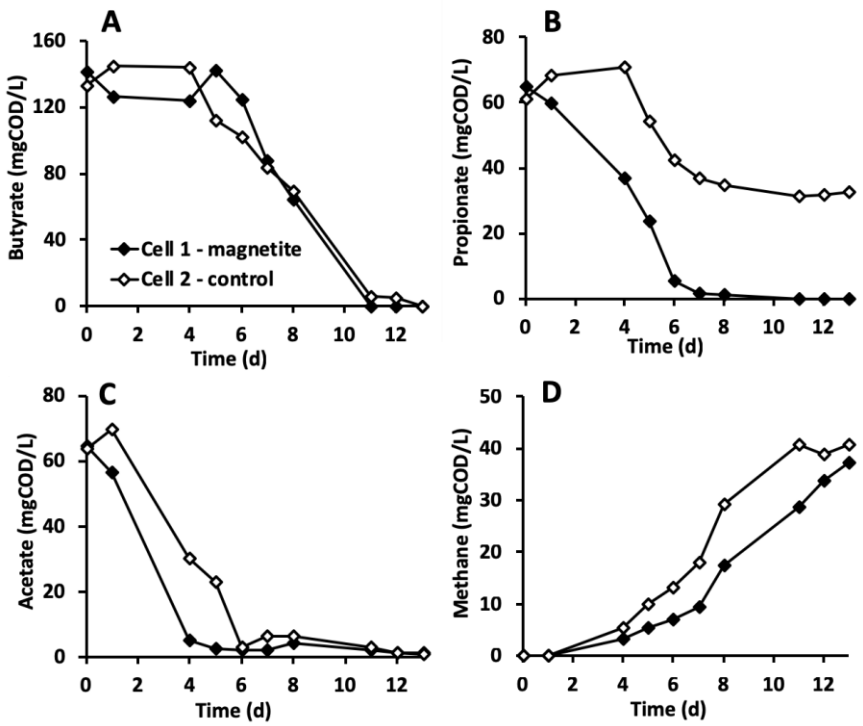

Figure 1. Bioelectrochemical oxidation of a mixture of VFAs (at E_{ANODE}= -0.1 V vs. SHE) (first feeding cycle) in the presence (Cell 1) and in the absence (Cell 2) of magnetite nanoparticles (250 mg Fe/L). Time course of butyrate (A), propionate (B), acetate (C) and methane (D) concentration (mgCOD/L).

After an initial lag phase of 5 days, butyrate started to be degraded, and was completely consumed, in both cells at similar rates, in approximately 11 days (Figure 1A). As far as propionate is concerned, it was rapidly and completely degraded in approximately 7 days, only in the cell containing magnetite

nanoparticles. By contrast, in the control cell (Cell 2), propionate degradation commenced only after a lag phase of 5 days and almost stopped when around 50% of the initial dose of substrate had been consumed (Figure 2B). As for acetate, it was rapidly and completely degraded in approximately 7 days in Cell 1, whereas degradation proceeded at a slightly lower rate in Cell 2 (Figure 1C). Methane was produced in both cells, although at a slightly higher rate in the control cell lacking magnetite nanoparticles (Figure 1D).

The higher rate and extent of acetate and propionate degradation in the cell supplemented with magnetite nanoparticles (Cell 1), were mirrored by a substantially higher electric current generation (Figure 2A). Notably, in Cell 1, the electric current reached a peak value of around 1.9 mA on day 4, which was nearly twice as much the highest value reached (on day 3) in Cell 2 (1 mA).

From day 5 till the end of the cycle, the electric current remained at lower (0.3 – 0.7 mA) and comparable values in both cells, in accordance with the similar rates of butyrate degradation. (Figure 2A). Irrespective of the presence of magnetite nanoparticles,at the end of the cycle, current generation accounted for a very high fraction(75-80%) of the removed substrate (Figure 2B). By contrast, methane production accounted for a minor share of the consumed substrate, namely 10% in Cell 2 and less than 5% in Cell 1 (Figure 2B).

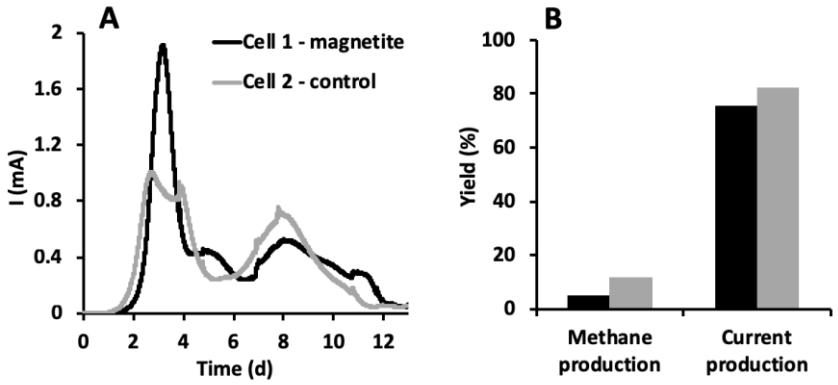

364

365 **Figure 2.**Electric current (A) and methane production and current production
366 yields (B) generated fromthe bioelectrochemical oxidation (at E_{ANODE}= -0.1 V vs.
367 SHE) (first cycle) of a mixture of VFAs in thepresence (Cell 1) and in the absence
368 (Cell 2) of magnetite nanoparticles (250 mg Fe/L).

369

370

371 In the second feeding cycle, the biodegradation of spiked VFAs proceeded at a
372 much higher rate(and without lag phases) with respect to the first feeding cycle,
373 clearly confirming the occurrence of microbial growth and/or acclimation of the
374 biomass on the supplied substrates (Figure 3). Interestingly, while butyrate and
375 acetate degradation (Figure 3A and 3C) now proceeded at similar rates in the two
376 bioelectrochemical cells, the biodegradation of propionate (Figure 3B) remained
377 greatly stimulated by the presence of magnetite nanoparticles, in agreement with
378 the result of the first feeding cycle. Besides enhancing propionate degradation,
379 magnetite nanoparticles slightly reduced methane production, also in accordance
380 with what observed during the first feeding cycle (Figure 3D).

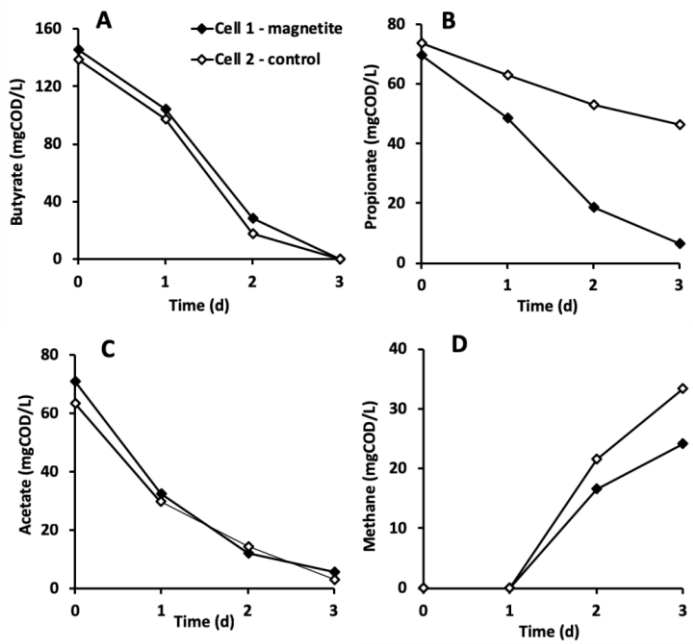

Figure 3. Bioelectrochemical oxidation of a mixture of VFAs (at E_{ANODE}= -0.1 V vs. SHE) (second cycle) in the presence (Cell 1) and in the absence (Cell 2) of magnetite nanoparticles (250 mg Fe/L). Time course of butyrate (A), propionate (B), acetate (C) and methane (D) concentration (mgCOD/L).

During the first 2 days of the second feeding cycle, the bioelectrochemical cells displayed very similar time profiles of electric current, in agreement with the fact that butyrate and acetate (which together accounted for nearly 75% of the total COD) degradation proceeded at similar rates. A positive effect of magnetite nanoparticles was apparent only from day 2 onward, hence when propionate degradation remained the main current-producing metabolism (Figure 4A).

Similarly to the first feeding cycle, both in the presence and in the absence of magnetite NPs, the yield of electric current generation (i.e., coulombic efficiency) computed at the end of the cycle was extremely high (80-90%) while the yield of methane production was lower than 10%.

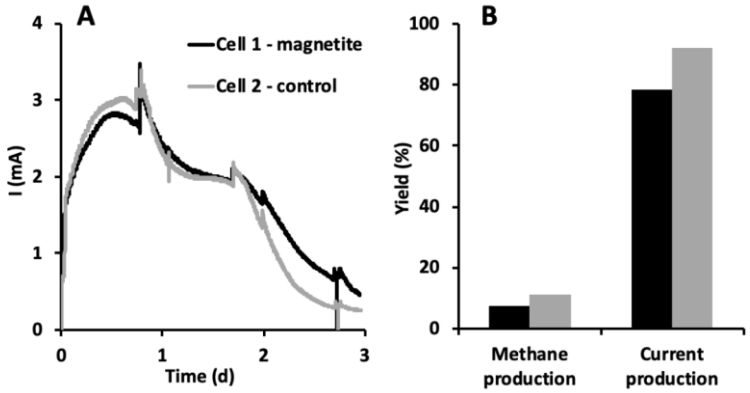

Figure 4. Electric current (A) and methane production and current production yields (B) generated fromthe bioelectrochemical oxidation (at E_{ANODE}= -0.1 V vs. SHE) (second cycle) of a mixture of VFAs in the presence (Cell 1) and in the absence (Cell 2) of magnetite nanoparticles (250 mg Fe/L).

In order to gain further insights into the effect of magnetite NPs on propionate degradation, during the third and fourth feeding cycle, propionate was spiked as the sole carbon source. During the third feeding cycle, the presence of magnetite, resulted in a 2-fold higher rate of propionate degradation (35 mgCOD/L d vs. 17 mgCOD/L d) (Figure 5A) and in a substantially reduced methane production (2.5

411 mgCOD/L d vs. 4.5 mgCOD/L d) (Figure 5B). As expected, the higher rate of
412 propionate oxidation in Cell1, was mirrored by a higher maximum electric current
413 generation (1.7 mA vs. 0.9 mA) (Figure 5C) and a slightly higher coulombic
414 efficiency (92% vs. 80%) (Figure 5D).During the fourth feeding cycle, the rate of
415 propionate degradation in the control cell (Cell 2) increased substantially (up to 28
416 mgCOD/L d) and almost reached that of Cell 1 (34 mgCOD/L d). Notably, this was
417 primarily due to an increase of methanogenic activity (from 4.5 mgCOD/L d during
418 cycle 3 to 21 mgCOD/L d during cycle 4), rather than of electrogenic activity,
419 thereby suggesting that propionate degradation was rate-limited by the electron-
420 scavenging activity of a syntrophic partner.Overall, an overview of the results of
421 the first set of batch experiments is summarized in Figure 6.
422 Finally, during the fifth feeding cycle, the bioelectrochemical cells were
423 supplemented again with the VFA mixture containing butyrate, propionate, and
424 acetate as carbon and energy sources. Notably, substrate utilization and electric
425 current generation were much higher than those observed during cycle 1 and 2,
426 and differences between Cell 1 and Cell2 were no more apparent (Figure 6),
427 possibly indicating that the kinetics of substrate utilization and current generation
428 became rate-limited by factors (e.g., the available electrode surface area and/or
429 mass transport phenomena) on which the magnetite nanoparticles had no effects.
430
431

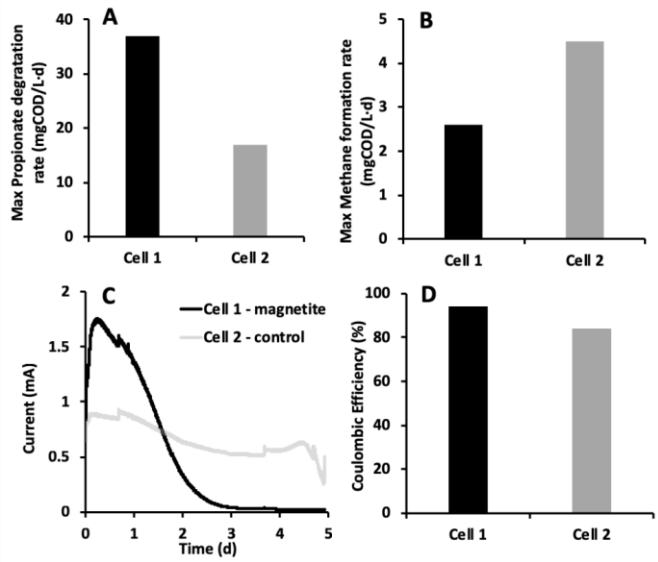

Figure 5. Bioelectrochemical oxidation of propionate (at E_{ANODE}= -0.1 V vs. SHE) in the presence (Cell 1) and in the absence (Cell 2) of magnetite nanoparticles (250 mg Fe/L): A) Maximum propionate degradation rate; B) Maximum methane formation rate; C) Electric current production; D) Coulombic efficiency.

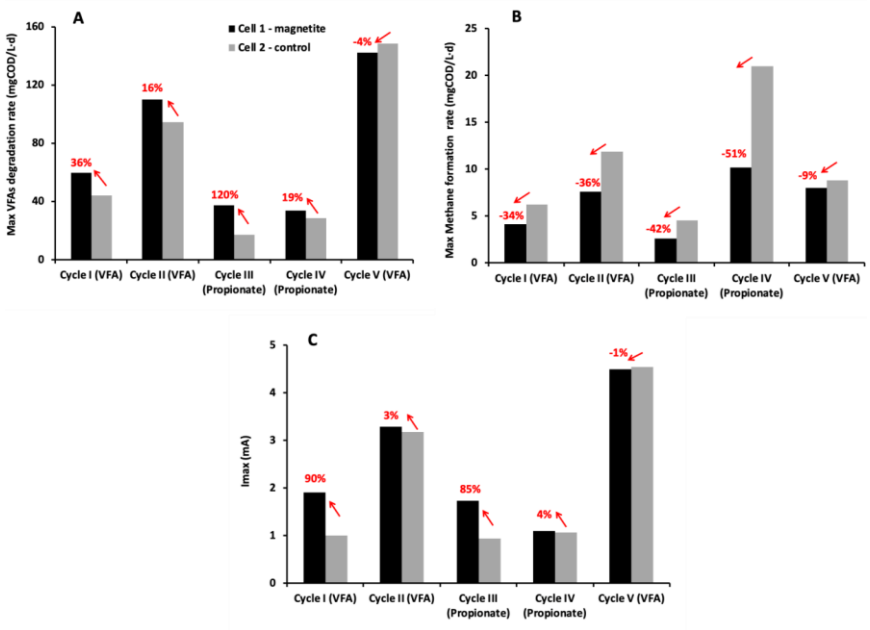

439

440 **Figure 6.**Overview of the first set of experiments conducted with the VFAs
441 mixture: A) Maximum VFAs degradation rate; B) Maximum methane formation
442 rate; C) Maximum electric current produced. Arrows highlight variations of
443 measured/calculated parameters triggered by the presence of magnetite
444 nanoparticles.

445

446

447 *3.2. Bioelectrochemical treatment of a synthetic municipal sewage*

448 In the second set of experiments, carried out on a freshly inoculated sludge, the
449 impact of magnetite NPs on the bioelectrochemical degradation of a synthetic
450 municipal sewage was examined. To this aim, two successive feeding cycles were

carried out, in which the bioelectrochemical cells were supplied with the synthetic sewage.

Regardless of the presence of magnetite, when the sewage was supplied as the sole carbon and energy source (cycles 1-2), the concentration of soluble COD displayed a first order decay (Figure 7A). In cycle 1, the calculated first-order kinetic coefficients were 0.13 (1/d) and 0.09 (1/d) for Cell 1 and Cell 2, respectively, hence providing a preliminary indication that magnetite NPs could enhancethe kinetics of sewage treatment. As expected, VFA, and particularly propionate (Figure 7B), transiently accumulated (up to a concentration of nearly 50 mgCOD/L) during the anaerobic treatment of the sewage. Importantly, as observed in the case of experiments with VFA as the spiked substrates, propionate was degraded more rapidly in the cell containing magnetite nanoparticles relative to the control (Figure 7B). The beneficial effect of magnetite nanoparticles was apparent also on electric current generation which increased more rapidly during the initial part of the cycle and reached a higher peak value (2.8 mA vs. 2.4 mA) in the cell containing magnetite nanoparticles, with respect to the control cell (Figure 7C). At the end of the cycle, the Coulombic efficiency was in the range 75-85 %, whereas the yield of methane production was lower than 25%, both in the presence and in the absence of magnetite NPs.

The positive effect of magnetite NPs was confirmed during cycle 2, whereby the estimated first-order kinetic coefficients for COD degradation in Cell 1 and Cell 2 were 0.40 (1/d) and 0.29 (1/d), respectively. The faster removal of COD was mirrored by a lower accumulation of total VFAs (24 mgCOD/L vs. 35 mgCOD/L, in Cell 1 and Cell 2, respectively) during sewage treatment and in their more rapid

consumption. Consistently, the corresponding peak values of electric current were 3.5 mA and 2.6 mA, for Cell 1 and Cell 2, respectively.

Importantly, as far as methane production is concerned, in Cell 1 (i.e., in the presence of magnetite NPs), the maximum rate of methane ~~of methane~~ production was 4% and 15% lower than in the control Cell 2, during the first and second feeding cycle with the synthetic sewage as the carbon and energy source.

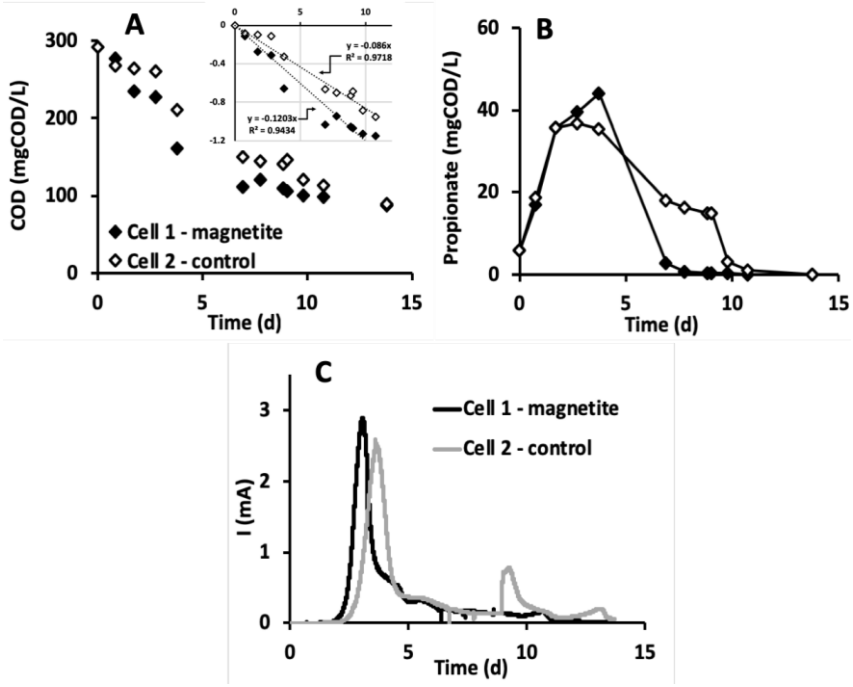

Figure 7. Bioelectrochemical oxidation of the OECD synthetic sewage (at E_{ANODE}= -0.1 V vs. SHE) in the presence (Cell 1) and in the absence (Cell 2) of magnetite nanoparticles (250 mg Fe/L).Time course of COD (A), propionate (B), and electric current production (C).

3.3. *Illumina Miseq sequencing of 16S rRNA gene analysis*

At the end of the I and II set of bioelectrochemical experiments, the anode biofilms and anolytes of cells supplemented or not with magnetite NPs were sampled for bacterial and archaeal ~~microbial~~ communities' analyses. The initial inocula were also analysed.

Table 1 shows Shannon indices for anode biofilms and anolytes from the cell supplemented with magnetite nanoparticles (Cell 1) and from the control cell (Cell 2) at the end of the first set (i.e., using VFAs mixture as substrate) and at the end of the second set (i.e., using the synthetic sewage) of experiments. The table shows that, in both sets of experiments, the anode biofilms and the biomass suspended in the anolytes of Cell 1 exhibited a slightly higher population diversity than those in Cell 2. Furthermore, as expected, due to the more complex composition of the sewage relative to the VFA mixture, the biomass diversity in the second set of experiments was substantially higher than in the first one.

Table 1. Shannon indices for anode biofilms (B) and biomass suspended in anolytes (A) in the presence (Cell 1) and in the absence (Cell 2) of magnetite nanoparticles.

	I set of experiments (VFAs mixture)				II set of experiments (OECD synthetic sewage)			
	Cell 1		Cell 2		Cell 1		Cell 2	
Sample type	B	A	B	A	B	A	B	A

Shannon indices	1.93	1.54	1.21	1.29	2.20	1.90	1.88	1.77

Figure 8 shows the phylum distribution of inoculum, anode biofilms and anolytes communities. Relative abundance at phylum level showed that all communities were dominated by representatives of six phyla: *Proteobacteria, Bacteroidetes, Firmicutes, Synergistetes, Chloroflexiand Spirochaetes*. Notably, the three phyla *Proteobacteria, Firmicutes*, and *Bacteroidetes* are frequentlyobserved at the anode of bioelectrochemical systems[9,10,42,43].

Samples coming from the first set of experiments (using the VFAs mixture as feed substrate) were highly dominated by *Proteobacteria* (63.76 – 86.86 %), both for the biofilms and anolytes communities, as well as the initial inoculum (Figure 8A). In spite of that, however, not significative differences at phylum level were observed in presence or absence of magnetite NPs.

By contrast, samples coming from the second set of experiments (i.e., using the synthetic sewage)were represented by *Bacteroidetes* (27.83-61.58%), *Synergistetes* (9.53 - 37.90%), and *Firmicutes* (9.19 -28.98%), both for the biofilms and anolytes communities (Figure 8B). It is noteworthy that anode biofilms from Cell 1 and Cell 2 were dominated by *Proteobacteria* (54.74 – 63.39 %), while in the anolytes there is a predominance of *Bacteriodetes*. Therefore, as expected the supplied organic substrates remarkably steered the community composition inbioelectrochemical systems.

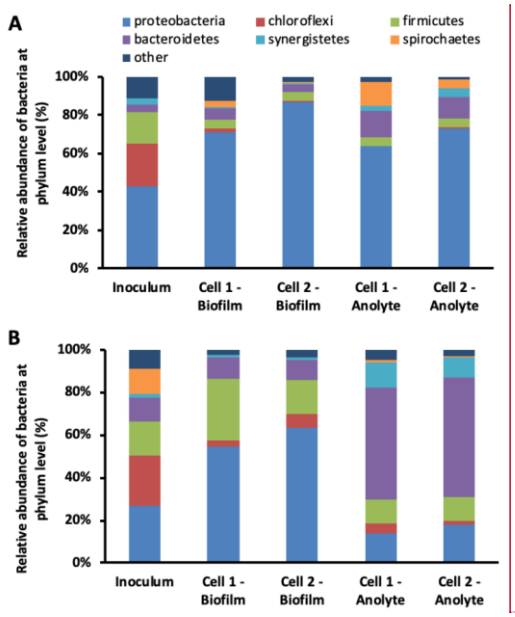

Commentato [HC4]: please put the names of the phyla in the legend in italics

Figure 8. Phylum distribution of the initial inoculum, anode biofilms and anolytes communities in the presence (Cell 1) and in the absence (Cell 2) of magnetite nanoparticles: A) first set of experiments with the VFAs mixture; B) second set of experiments with the OECD synthetic sewage.

Figure 9 shows the relative abundance of bacteria in the inoculum, anode biofilms and anolytes at species level. The inoculum used in the first set of experiments was represented by various species, with a predominance of *Pseudomonas spp.* (about 30%) and *Bellilinea spp.* (about 13%). Samples coming from the first set of experiments revealed that anode biofilms both in Cell 1 and Cell2 became largely dominated by *Proteobacteria* including the well-known electro-active and Fe(III)-reducing bacteria such as *Geobacter* (*G. sulfurreducens* and *G. metallireducens*)

which represented at least 83.5 % and 65% of the biofilm communities, respectively. The other part of the community was made up of various species, the percentage of each being typically always less than 2%, except *Eggertella spp* (9.45%) detected in the bioanode of Cell 1 (Figure 9A). Anolytes from Cell 1 and Cell 2 were both dominated by *Rhodopseudomonas palustris* (55-65%). Interestingly, a strain of *R. palustris* (DX-1) is one of the few *Alphaproteobacteria* found to generate electricity at high power densities from VFAs and alcohols [44].

Samples from the second set of experiments (i.e., using the OECD synthetic sewage as feed substrate) gave similar results about the relative abundance of bacteria on bioanodes, whereby *Geobacter* species accounted for 48-57% of biofilm communities in the presence and in the absence of magnetite. However, the bacterial ~~microbial~~ communities on the anodes of the second set of experiments clearly differed from those of the first set. In fact, besides *Geobacter*, anode biofilms also included *Desulfuromonas* (11.3 – 3.8%), *Clostridium* (14.4- 8.1%) and *Bacteroides* (6.1 – 7.2%) species, respectively (Figure 9B). Importantly, microorganisms belonging to these genera were all previously reported to exhibit exoelectrogenic activity[10]. Anolytes from Cell 1 and Cell 2 were both dominated by *Rikenella sp.* (35-40%), *Parabacteroides spp.* (10%) and *Synergistes spp*. (10%).

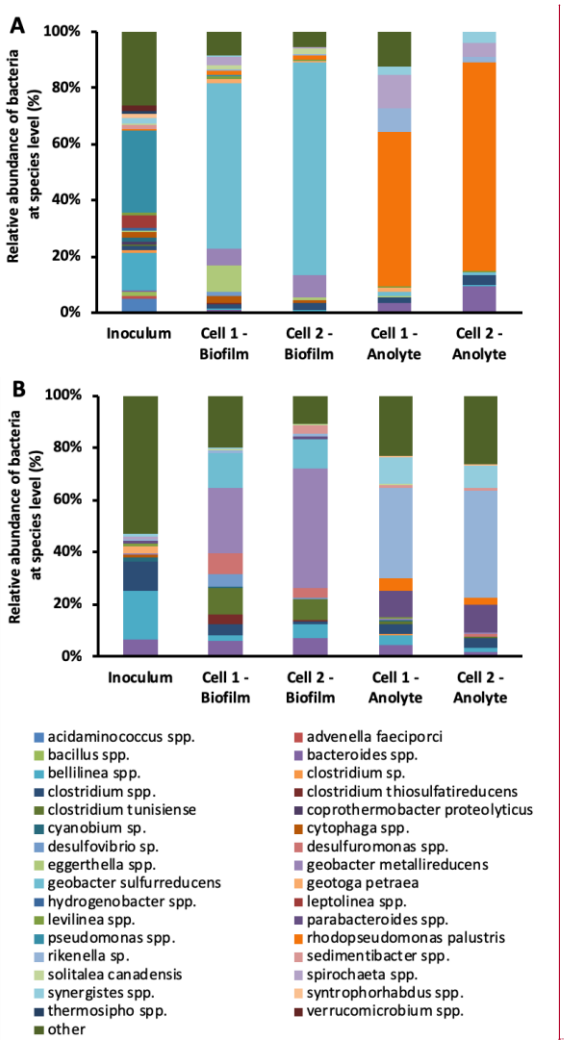

Commentato [HC5]:
i)in this figure there are too many legends. It is very hard to match the colors to species. May be we should label the main species on the bar chart directly, or leave only the most abundant species
ii) please put the names species in the legend in italics

xxx

Commentato [HC6]: I sent results of the analysis of the archaea, especially methanogenic strains that I can't find here. this data is very interesting in our study!

Figure 9. Relative abundance of bacteria at level species of the initial inoculum (I), anode biofilms (Bi) and anolytes (Ai) communities in the presence (Cell 1) and in the absence (Cell 2) of magnetite nanoparticles: A) first set of experiments with the VFAs mixture; B) second set of experiments with the OECD synthetic sewage.

4. Discussion

The results of this study highlighted the potential of magnetite NPs in improving the performance of microbial electrochemical technologies, aimed at energy recovery from sewage treatment. The improvement primarily resulted from the acceleration of the electrogenic oxidation of organic constituents of the sewage, and particularly propionate. The observed effect of magnetite NPs on propionate degradation is consistent with the fact that this compound, which is a central metabolite in the anaerobic (methanogenic) degradation of organic matter, requires the syntrophic cooperation of acetogenic bacteria and methanogenic archaea (or of other electron-scavenging microorganisms) to be effectively degraded. For this reason, propionate accumulation in anaerobic digesters is typically regarded as an indicator of inefficient degradation and possibly of process failure. Typically, acetogenic bacteria oxidize propionate into acetic acid and H_2 (or formate), according to the following reaction: $Propionate^- + 3H_2O \rightarrow Acetate^- + HCO_3^- + H^+ + 3H_2$. Under standard biochemical conditions this reaction is energetically unfavorable ($\Delta G' = +76.1$ kJ/mol) and therefore becomes only possible (i.e., $\Delta G'<0$) if the products, acetate and particularly H_2, are kept at low concentration levels by the scavenging activity of acetoclastic and hydrogenophilic methanogenic Archaea and/or of other electron-scavenging microorganisms such as the EAB.

Since in the herein reported bioelectrochemical experiments, the presence of magnetite had only little effects on acetate concentration profiles, it is likely that

NPs directly or indirectly affected the scavenging of electrons (and/or of H_2) deriving from propionate oxidation, according to the mechanisms depicted in Figure 9.

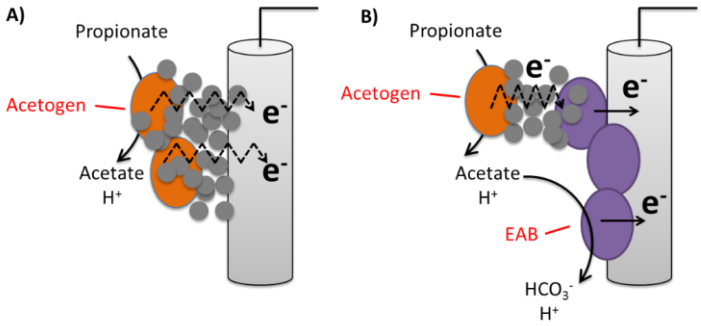

Figure 9. Hypothetical mechanisms underpinning the effect of magnetite NPs on propionate degradation: A) transfer of electrons coming from propionate oxidation to the electrode through magnetite NPs; B) transfer of electrons coming from propionate oxidation to EAB through magnetite NPs.

In the first hypothetical mechanism (Figure 9A), the electrons coming from propionate oxidation are transferred from the acetogen directly to the electrode, hence preventing the intermediate H_2 generation, with the magnetite NPs serving as electron conduits.

In the second hypothetical mechanism (Figure 9B), the electrons released from propionate oxidation are transferred to EAB via a magnetite-driven interspecies

electron transfer mechanism. Ultimately, EAB discharge the received electrons to the electrode by using it as the terminal respiratory electron acceptor.

Overall, in both cases magnetite NPs facilitate the microbial community using the anode as an alternative sink for electrons deriving from propionate degradation, thereby accelerating substrate degradation and electric current generation.

Nonetheless, it cannot be ruled out that magnetite NPs also facilitated the transfer of electrons to the electrode by increasing the electrical conductivity of the microbial biofilm growing on the electrode surface, and in turn reducing the resistance to electron transfer.

A major finding of this study is the positive effect of magnetite NPs also on the bioelectrochemical treatment of a synthetic sewage of complex composition. Analogously to what observed when a mixture of VFA was supplied as the carbon and energy source, also with the synthetic sewage propionate degradation was found to be accelerated, confirming the positive role of magnetite NPs in facilitating the oxidation of substrates and metabolites whose anaerobic degradation requires a syntrophic cooperation among microorganisms. Along this line it is plausible that the same effect occurred also for other, yet unidentified, constituents of the synthetic sewage such as lipids and proteins. Clearly, further work is needed to verify this hypothesis.

Interestingly, magnetite NPs reduced (up to 50%) the maximum observed rate of methane production (i.e., a parasitic reaction in competition with the generation of electric current), also when as synthetic sewage of complex composition was used as the sole carbon and energy source. This finding is consistent with the hypothesis that in the presence of magnetite the degradation of organic substrates proceeds

without or with lower intermediate accumulation of H_2, a direct substrate of methanogens, although this aspect will also have to be experimentally confirmed in future studies.

In conclusion, this study demonstrated for the first time that addition of little amounts of magnetite nanoparticles can be an effective strategy to kick-start a bioelectrochemical system designed for wastewater treatment and improve, at least on a short-term scale, the effectiveness of electrogenic substrate oxidation processes. Future studies will have to identify the optimal strategy of magnetite addition as well as the long-term efficacy of the proposed approach.

Acknowledgements

This study was financially supported by MIUR (the Italian Ministry of University and Research) and the MESRS (Ministry of High Education and Scientific Research of the Tunisian Republic, grant number LR11ES31) in the frame of the WE-MET Project (ERANETMED_NEXUS-14-035).

Formattato: Tipo di carattere: Cambria

652

653 **References**

654 1 E. S. Heidrich, T. P. Curtis and J. Dolfing, *Environ. Sci. Technol.*, 2011, **45**, 827–
655 832.

656 2 F. Harnisch, F. Aulenta and U. Schröder, in *Comprehensive Biotechnology*,
657 Elsevier, 2011, vol. 1, pp. 643–659.

658 3 P. L. McCarty, J. Bae and J. Kim, *Environ. Sci. Technol.*, 2011, **45**, 7100–7106.

659 4 L. Appels, J. Lauwers, J. Degrève, L. Helsen, B. Lievens, K. Willems, J. Van Impe
660 and R. Dewil, *Renew. Sustain. Energy Rev.*, 2011, **15**, 4295–4301.

661 5 T. A. Elmitwalli, K. L. T. Oahn, G. Zeeman and G. Lettinga, *Water Res.*, 2002,
662 **36**, 2225–2232.

663 6 R. M. McKeown, D. Hughes, G. Collins, T. Mahony and V. O'Flaherty, *Curr.*
664 *Opin. Biotechnol.*, 2012, **23**, 444–451.

665 7 K. Rabaey and R. A. Rozendal, *Nat. Rev. Microbiol.*, 2010, **8**, 706–716.

666 8 H. Wang, H. Luo, P. H. Fallgren, S. Jin and Z. J. Ren, *Biotechnol. Adv.*, 2015, **33**,
667 317–34.

668 9 B. E. Logan, R. Rossi, A. Ragab and P. E. Saikaly, *Nat. Rev. Microbiol.*, 2019, 1.

669 10 B. E. Logan, *Nat. Rev. Microbiol.*, 2009, **7**, 375–381.

670 11 Y. Zhang and I. Angelidaki, *Water Res.*, 2014, **56**, 11–25.

671 12 B. E. Logan, D. Call, S. Cheng, H. V. M. Hamelers, T. H. J. A. Sleutels, A. W.
672 Jeremiasse and R. A. Rozendal, *Environ. Sci. Technol.*, 2008, **42**, 8630–8640.

13 M. Villano, F. Aulenta, C. Ciucci, T. Ferri, A. Giuliano and M. Majone, *Bioresour. Technol.*, 2010, **101**, 3085–3090.

14 S. Cheng, D. Xing, D. F. Call and B. E. Logan, *Environ. Sci. Technol.*, 2009, **43**, 3953–3958.

15 D. F. Call and B. E. Logan, *Appl. Environ. Microbiol.*, 2011, **77**, 8791–8794.

16 A. M. Speers and G. Reguera, *Appl. Environ. Microbiol.*, 2012, **78**, 437–444.

17 P. D. Kiely, J. M. Regan and B. E. Logan, *Curr. Opin. Biotechnol.*, 2011, **22**, 378–385.

18 P. Parameswaran, C. I. Torres, H.-S. Lee, R. Krajmalnik-Brown and B. E. Rittmann, *Biotechnol. Bioeng.*, 2009, **103**, 513–23.

19 U. Schroeder and F. Harnisch, in *Encyclopedia of Applied Electrochemistry*, Springer New York, New York, NY, 2014, pp. 120–126.

20 P. Choudhury, U. S. Prasad Uday, T. K. Bandyopadhyay, R. N. Ray and B. Bhunia, *Bioengineered*, 2017, **8**, 471–487.

21 R. Nitisoravut, C. N. D. Thanh and R. Regmi, *Int. J. Green Energy*, 2017, **14**, 712–723.

22 D. R. Lovley, *Annu. Rev. Microbiol.*, 2017, **71**, annurev-micro-030117-020420.

23 S. Kato, K. Hashimoto and K. Watanabe, *Proc. Natl. Acad. Sci.*, 2012, **109**, 10042–10046.

24 P. M. Shrestha and A.-E. Rotaru, *Front. Microbiol.*, 2014, **5**.

25 Q. Cheng and D. F. Call, *Environ. Sci. Process. Impacts*, 2016, **18**, 968–980.

26 C. Cruz Viggi, S. Rossetti, S. Fazi, P. Paiano, M. Majone and F. Aulenta, *Environ. Sci. Technol.*, 2014, **48**, 7536–7543.

27 S. Chen, A.-E. Rotaru, P. M. Shrestha, N. S. Malvankar, F. Liu, W. Fan, K. P. Nevin and D. R. Lovley, *Sci. Rep.*, 2015, **4**, 5019.

28 Z. M. Summers, H. E. Fogarty, C. Leang, A. E. Franks, N. S. Malvankar and D. R. Lovley, *Science (80-.).*, 2010, **330**, 1413–1415.

29 S. Kato, K. Hashimoto and K. Watanabe, *Microbes Environ.*, 2013, **28**, 141–148.

30 M. A. Gacitúa, B. González, M. Majone and F. Aulenta, *Int. J. Hydrogen Energy*, 2014, **39**, 14540–14545.

31 Y. S. Kang, S. Risbud, J. F. Rabolt and P. Stroeve, *Chem. Mater.*, 1996, **8**, 2209–2211.

32 B. Tonanzi, A. Gallipoli, A. Gianico, D. Montecchio, P. Pagliaccia, M. Di Carlo, S. Rossetti and C. M. Braguglia, *Biomass and Bioenergy*, 2018, **118**, 55–64.

33 P. Leitão, S. Rossetti, H. P. A. Nouws, A. S. Danko, M. Majone and F. Aulenta, *Bioresour. Technol.*, 2015, **195**, 78–82.

34 K. B. Gregory, D. R. Bond and D. R. Lovley, *Environ. Microbiol.*, 2004, **6**, 596–604.

35 W. E. Balch, G. E. Fox, L. J. Magrum, C. R. Woese and R. S. Wolfe, *Microbiol. Rev.*, 1979, **43**, 260–296.

36 J. G. Zeikus, *Bacteriol. Rev.*, 1977, **41**, 514–541.

37 OECD, *Oecd Guidel. 303 Test. Chem.*, 2001.

38 APHA, *Standard Methods for Examination of Water and Wastewater*, 1999.

39 R. Amann, *FEMS Microbiol. Ecol.*, 1998, **25**, 205–215.

40 A. Loy, M. Horn and M. Wagner, *Nucleic Acids Res.*, 2003, **31**, 514–516.

41 G. Lupini, L. Proia, M. Di Maio, S. Amalfitano and S. Fazi, *J. Microbiol. Methods*, 2011, **86**, 248–251.

42 A. P. Borole, G. Reguera, B. Ringeisen, Z.-W. Wang, Y. Feng and B. H. Kim, *Energy Environ. Sci.*, 2011, **4**, 4813–4834.

43 R. Kumar, L. Singh and A. W. Zularisam, *Renew. Sustain. Energy Rev.*, 2016, **56**, 1322–1336.

44 D. Xing, Y. Zuo, S. Cheng, J. M. Regan and B. E. Logan, *Environ. Sci. Technol.*, 2008, **42**, 4146–4151.